Res Chem Intermed (2018) 44:4259–4276
https://doi.org/10.1007/s11164-018-3367-3

Synthesis and characterization of oxo-vanadium complex anchored onto SBA-15 as a green, novel and reusable nanocatalyst for the oxidation of sulfides and oxidative coupling of thiols

Taiebeh Tamoradi[1] · Mohammad Ghadermazi[1] · Arash Ghorbani-Choghamarani[2] · Somayeh Molaei[1]

Received: 4 December 2017 / Accepted: 1 March 2018 / Published online: 9 March 2018
© Springer Science+Business Media B.V., part of Springer Nature 2018

Abstract The present work describes the synthesis of a new oxo-vanadium complex immobilized on SBA-15 nanostructure as an efficient catalyst for oxidation of sulfides and oxidative coupling of thiols. Characterization of the resultant AMPD@SBA-15 nanostructure was performed by various physico-chemical techniques such as Fourier transform infrared spectroscopy, transmission and scanning electron microscopies, energy-dispersive X-ray spectroscopy, inductively coupled plasma optical emission spectroscopy, X-ray diffraction, thermal gravimetric analysis, and N_2 adsorption and desorption. The results of the developed procedure bring several benefits such as the use of commercially available, ecologically benign, operational simplicity, and cheap and chemically inert reagents. It shows good reaction times, practicability and high efficiency, and is easily recovered from the reaction mixture by simple filtration and reused for several consecutive cycles without noticeable change in its catalytic activity. More importantly, high efficiency, simple and an inexpensive procedure, commercially available materials, easy separation, and an eco-friendly procedure are the several advantages of the currently employed heterogeneous catalytic system.

✉ Taiebeh Tamoradi
t.tabss@yahoo.com

✉ Mohammad Ghadermazi
mghadermazi@yahoo.com

✉ Arash Ghorbani-Choghamarani
arashghch58@yahoo.com; arashghch@gmail.com; a.ghorbani@ilam.ac.ir

[1] Department of Chemistry, Faculty of Science, University of Kurdistan, Sanandaj, Iran

[2] Department of Chemistry, Faculty of Science, Ilam University, P.O. Box 69315516, Ilam, Iran

Graphical Abstract

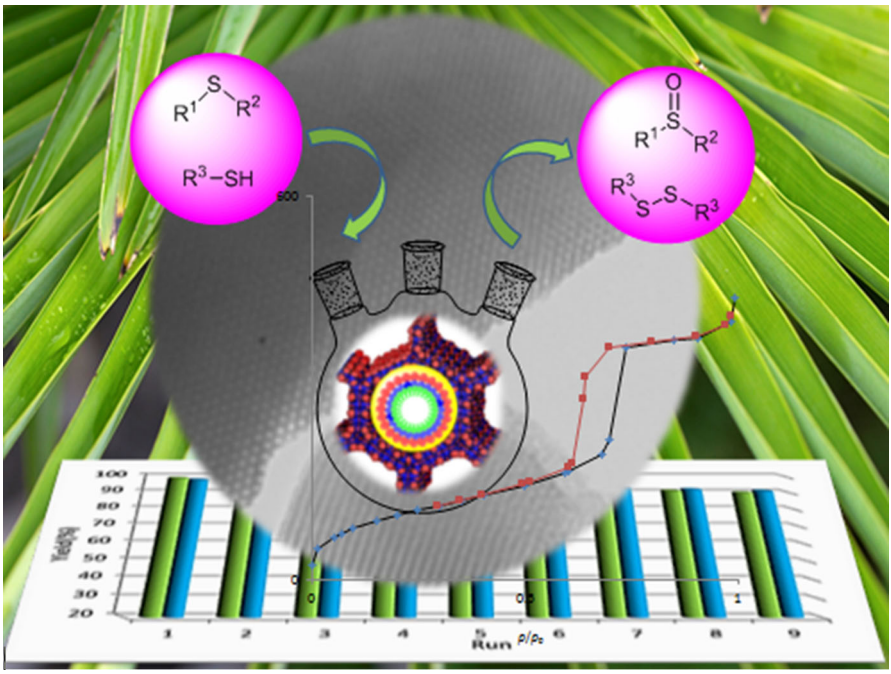

Keywords SBA-15 · Vanadium complex · Oxidation reaction · Sulfoxide · Disulfide

Introduction

In recent years heterogeneous catalysts are more important because of their recyclability, performance in activity and separation [1]. A homogeneous catalyst can be converted to a heterogeneous catalyst through support, such as organic and inorganic acids and bases supported on alumina, zeolite, silica gel, carbon nanotubes and magnetic nanoparticles. Supporting action modulates the performance of homogeneous catalysts in terms of selectivity and catalytic activity. It also makes all the beneficial properties of solid catalysts, such as easy separation and recycling available on homogeneous catalysts [2–6]. Among the existing substrates, those in nano levels are better candidates for the support of homogeneous catalysts due to their advantages such as very small size, which produces a high surface to volume ratio [7–9]. The use of pre-fabricated large porosity silicates has recently attracted the attention of researchers. Among these are the mesoporous patterns such as MCM-48, MCM-41 and SBA-15 [10]. Large porosities (Mesopores) are nanoparticles of diameter (2–50 nm) and have good properties such as high surface absorption, high specific surface, structural order and narrow pore distribution.

Meanwhile, SBA-15 mesoporous silica with a high specific surface area (about 782.46 m^2/g), cavity size (normally 4–6 nm), and high thermal resistance, is known as the best large porosity silica with two-dimensional symmetry having equal ventures with hexagonal arrangement [11]. Oxidation of sulfides and thiols are important reactions in organic chemistry [12], they are used as valuable synthetic intermediates in the production of a wide range of chemicals, active molecules and pharmaceuticals [13, 14]. Certain sulfoxicides play an important role in antifungal, anti-hypertensive and vasodilator drugs [15–17]. The rich chemistry of sulfoxides makes them highly useful reagents in syntheses. Sulfoxides are interesting active groups that are widely used to form carbon–carbon bonds, especially in organic reactions, and the transformation of functional groups and molecular redistribution [18]. On the other hand, the formation of disulfide bonding in peptides and active biochemical molecules, as well as in the processing of sweet oil, is important. The low sulfur-sulfur bond leads to high reactivity of these compounds. Additionally, in the chemical and industrial fields, disulfides are used as a volcanizing agent for rubbers and elastomers, as well as modifying the surface of precious metals such as gold, silver, platinum, palladium and some semiconductors [19, 20]. Among methods for synthesizing sulfoxides and disulfide, the oxidation of sulfides and thiols to the corresponding sulfoxides and disulfide is very common and, of course, desirable. The study of different oxidation methods shows that the attention of chemists is more to achieve superior methods than the old ones. These methods are more appropriate in terms of reaction time, greater yield, easier product separation, and they are cheaper and more selective. Herein, new oxovanadium complex immobilized on SBA-15 has been reported as a recoverable nanocatalyst for the oxidation of sulfides to sulfoxides and oxidative coupling of thiols into corresponding disulfides under neat conditions.

Experimental

General

The cationic surfactant Pluronic P123 triblock copolymer ($EO_{20}PO_{70}EO_{20}$, MW 5800), tetraethyl orthosilicate (TEOS; 98%), 3-chloropropyltrimethoxysilane (CPTMS), triethylamine, ethanol, ethyl acetate, acetonitrile, H_2O_2 (33%), n-Hexane, vanadyl acetylacetonate ($VO(acac)_2$), toluene, 2-amino-2-methyl-1,3-propanediol (AMPD) and all reagents were purchased from Merck, Sigma-Aldrich and Fluka. IR spectra were examined for characterization of prepared samples by KBr disc using a VERTEX 70 model BRUKER FT-IR spectrophotometer. Powder X-ray diffraction (XRD) patterns were collected to obtain the crystallographic structure of nanocatalysts by X-ray diffraction patterns using a Cu radiation source with a wavelength λ = 1.54060 Å, 40 kV. SEM and TEM images were recorded using FESEM-TESCAN $MIRA_3$ and Zeiss-EM10C TEM, respectively. The thermal stability of the nanocatalyst was also studied by TGA using a Shimadzu DTG-60 instrument in the temperature range of 50–750 °C. Melting points of products were determined with an Electrothermal 9100 apparatus. Inductively coupled plasma

optical emission spectrometry (ICP-OES) was used to obtain the vanadium content of the nanocatalyst.

General procedure for the preparation of the VO-AMPD@SBA-15

The SBA-15 mesoporous silica has been successfully prepared according to a very recently reported method [21]. Initially, SBA-15 nanoparticles were prepared by adding 4g of pluronic 123 as the surfactant template to a solution containing 90 mL of HCl solution (2 M) and deionized water (30 mL). The resulting mixture was stirred at 35 °C for 5 h, and then 9.04 mL of tetraethylorthosilicate (TEOS) as the silica source was gradually added to the solution, and the mixture stirred at the same temperature for 20 h. Finally, the collected product was washed with deionized water followed by calcination at 823 K for 5 h at a rate of 2 °C/min to remove the residual surfactants. The white powders were designated that affords pure silica SBA-15. Then, 1 g of the obtained SBA-15 with 1.5 mL of 3-chloropropyltrimethoxysilane (CPTMS) refluxed in dry toluene (20 mL) for 24 h. The final product was separated by simple filtration, washed with hexane and dried at 50 °C to give the SBA-15 coated with CPTMS. AMPD@SBA-15. nanoparticles were subsequently produced by the reaction of the CPTMS supported on SBA-15 (1 g) with 0.21 g of 2-Amino-2-methyl-1,3-propanediol (AMPD) and triethylamine (1.5 mmol) in dry toluene under reflux conditions for 48 h. AMPD@SBA-15 was separated by filtration, washed with deionized water and ethanol and dried at 50 °C. Then, VO-AMPD@SBA-15 was successfully obtained through coordination of AMPD@SBA-15 ligand with vanadium. Furthermore, AMPD@SBA-15 (1 g) and $VO(acac)_2$ (0.672 g) were mixed in 30 mL ethanol, and then the mixture was refluxed for 16 h. The nanosolid VO-AMPD@SBA-15 was separated from the solution by filtration. The final product was washed with copious amounts of ethanol and dried under vacuum at room temperature.

General procedure for the oxidation of sulfides

In a typical experimental procedure, a round-bottomed flask was charged with sulfide (1 mmol), H_2O_2 (30% aqueous, 0.3 mL) and VO-AMPD@SBA-15 (0.004 g). Then the mixture was stirred at room temperature under solvent-free conditions and the progress of the reaction was monitored by TLC. After completion of the reaction, the catalyst was removed by filtration, and the residue was extracted with ethyl acetate. The organic extract was dried over anhydrous Na_2SO_4 then evaporated to give the desired product without further purification.

General procedure for the oxidation of thiols to disulfides

In another study, a mixture of the VO-AMPD@SBA-15 (0.004 g), thiol (1 mmol) and H_2O_2 (0.4 mL) was stirred at room temperature in ethyl acetate (2 mL). The progress was monitored by TLC. After completion of the reaction, VO-AMPD@SBA-15 catalyst was separated from the mixture by filtration. Then

products were extracted with ethyl acetate and dried, and the solvent was removed to give the pure disulfides.

Results and discussion

Catalyst preparation

Briefly, 3 chloropropyltrimethoxysilane was first loaded on the surface of SBA-15 nanoparticles. Then surfaces of Sba-15 nanoparticles were coated using 2-amino-2-methyl-1,3-propanediol (AMPD) ligand as a green and available diol by reaction of chloride groups of CPTMS supported on SBA-15 nanoparticles and amine groups of AMPD ligand. Finally, treatment of AMPD@SBA-15 with $VO(acac)_2$ provides VO-AMPD@SBA-15through a stable interaction between the metal ions and functional groups of the diol (Scheme 1).

Catalyst characterization

SEM images of VO-AMPD@SBA-15 are depicted in Fig. 1. According to these images, micrographs of the prepared samples show uniform particle size distribution and particles with diameters of about 300 nm, retaining the well-defined wheat-like macrostructure clusters of pure SBA-15.

The TGA curve of the VO-AMPD@SBA-15 shows the quantitative determination of the organic groups decreases supported on the surface of SBA-15 nanostructure. It should be noted that the mass of the organic functional groups decomposes upon heating. As shown in Fig. 2, the small amount of weight loss happens below 200 °C, which is due to removal of physically adsorbed solvent and surface hydroxyl groups, and the other weight loss of about 27% between 200 and 600 °C is related to decomposition of functional groups chemisorbed onto the surface of SBA-15 nanoparticles [22]. On the basis of the results of the TGA curve,

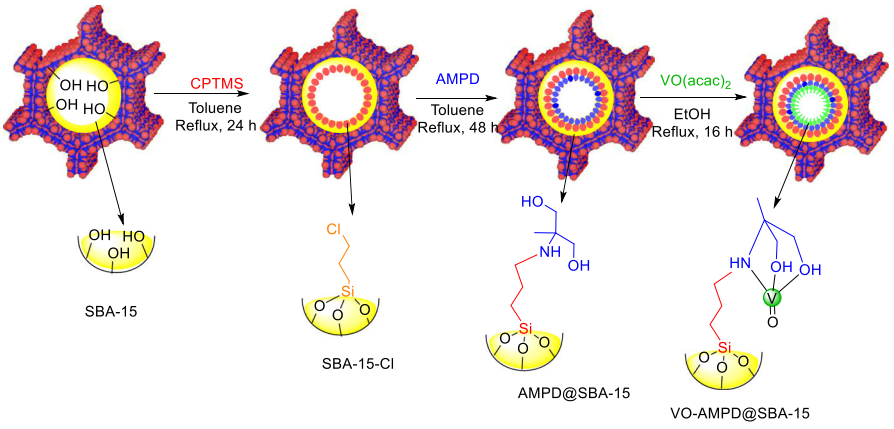

Scheme 1 Synthesis of VO-AMPD@SBA-15 nanocatalyst

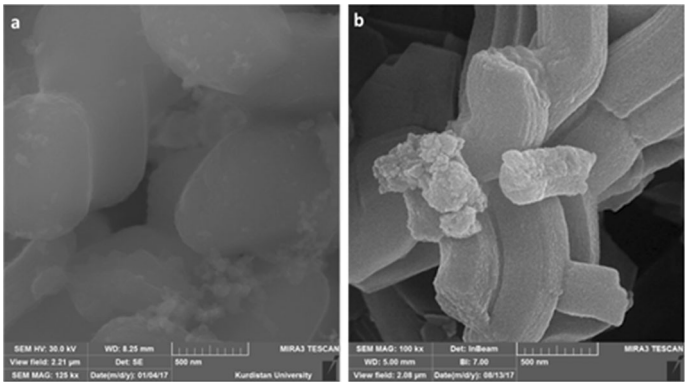

Fig. 1 SEM image of calcined SBA-15 (**a**) and SEM images of VO-AMPD@SBA-15 (**b**)

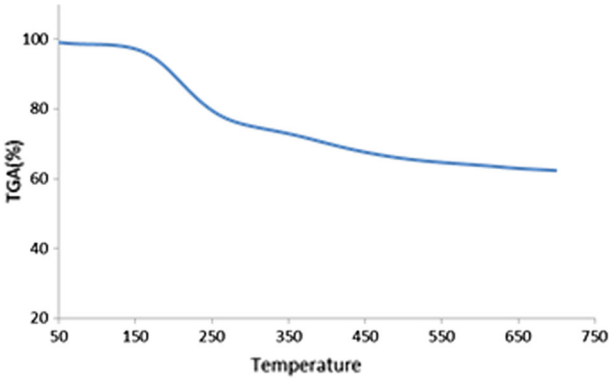

Fig. 2 TGA thermogram of VO-AMPD@SBA-15

the well grafting of vanadium 2-Amino-2-methyl-1,3-propanediol complex onto mesoporous SBA-15 silica is verified.

One indication of bond formation between the nanoparticles and the vanadium complex can be inferred from FTIR. FTIR spectra within the range of 400–4000 nm for SBA-15, SBA-15-Cl, AMPD@SBA-15 and VO-AMPD@SBA-15 nanoparticles were demonstrated (Fig. 3). As shown in Fig. 3a, the FTIR spectrum of the SBA-15 sample displays characteristic absorption peaks at 1099, 842 and 480 cm^{-1} corresponding to Si&bond;O&bond;Si asymmetric stretching, Si&bond;O&bond;Si symmetric stretching and Si&bond;O&bond;Si bending vibrations, respectively. Also, the presence of C&bond;H stretching vibration at 2912 cm^{-1} in the SBA-15-Cl spectrum is due to the anchored (3-choloropropyl) trimethoxysilane [23]. Furthermore, in the spectrum of AMPD@SBA-15, bands in the range of 1550 and 13,250 cm^{-1} are attributed to the N–H and C–N vibrations, confirming grafting of the organic groups onto the SBA-15 nanoparticles. Also, in order to determine the exact amount of vanadium loaded on modified magnetic nanoparticles, ICP-OES analysis was performed, and it was found to be 0.41 mmol g^{-1}.

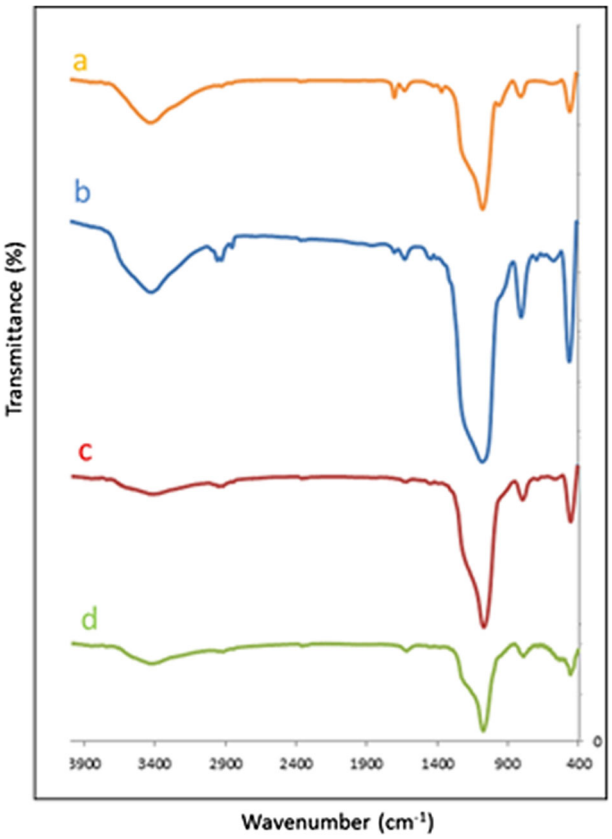

Fig. 3 FTIR spectrum of bare SBA-15 nanoparticles, SBA-15-Cl, AMPD@SBA-15 and VO-AMPD@SBA-15

TEM images of VO-AMPD@SBA-15 at different magnifications are depicted in Fig. 4. It can be seen that the catalyst was formed of nanometer-sized particles. It should be mentioned that the images are indicative of uniform particle size and hexagonal shape.

The N_2 adsorption/desorption isotherm for VO-AMPD@SBA-15 nanocatalyst is shown in Fig. 5. As seen in Table 1, the Brunauer–Emmett–Teller surface area (S_{BET}), the Barret–Joyner–Halenda average pore diameter (DBJH) and the total pore volumes (V_{total}) of VO-AMPD@SBA-15 are summarized. It can be seen that a decrease in the SBET, DBJH and Vtotal for VO-AMPD@SBA-15 nanocatalyst upon post anchoring of vanadium complex on the wall of functionalized SBA-15 was observed, which is due to the presence of a pendant group on the pore surface that partially blocks the adsorption of nitrogen molecules [24]. Also, the N_2 adsorption/desorption isotherm of SBA-15 and VO-AMPD@SBA-15 indicated that the texture of initial material of the SBA-15 upon post anchoring of vanadium complex on SBA-15 was retained.

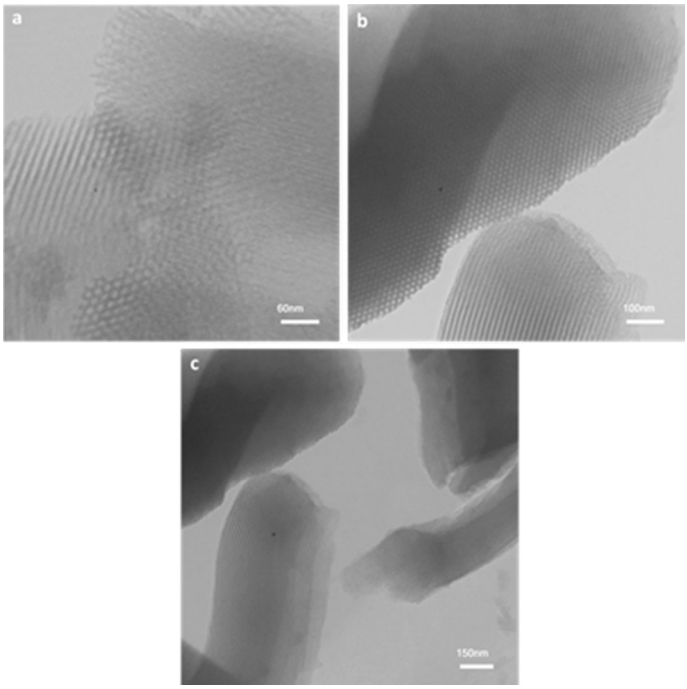

Fig. 4 TEM images of VO-AMPD@SBA-15 catalyst at different magnifications (a, b and c)

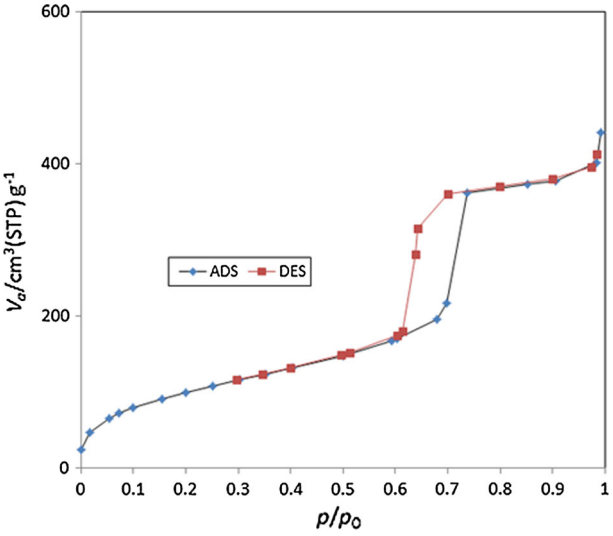

Fig. 5 Nitrogen adsorption/desorption isotherms of VO-AMPD@SBA-15

Table 1 Texture parameters obtained from nitrogen adsorption studies

Sample	SBET (m^2 g^{-1})	Pore diameter by BJH method (nm)	Pore volume (cm^3 g^{-1})
SBA-15	874	6.168	1.049 [24]
VO-AMPD@SBA-15	360.19	3.52	0.662

The crystalline structures of the VO-AMPD@SBA-15 catalyst were determined by powder X-ray diffraction (XRD). The peak positions in the sample remained constant after the functionalization process as compared to the SBA-15. The intense peak corresponding to the pore family and the two additional weak reflections assigned to the family planes, which are indicative as (100), (110), and (200) reflections are associated with a hexagonal space group symmetry P6mm and high hexagonal mesoscopic order (Fig. 6) [23].

Catalytic studies

In this research, we developed the preparation of a recyclable, green and efficient nanocatalyst. Then, in order to investigate the catalytic activity of the prepared nanohybrid, we investigated it for the oxidation of sulfides (Scheme 2) and oxidative coupling of thiols (Scheme 3). In this regard, the oxidation of

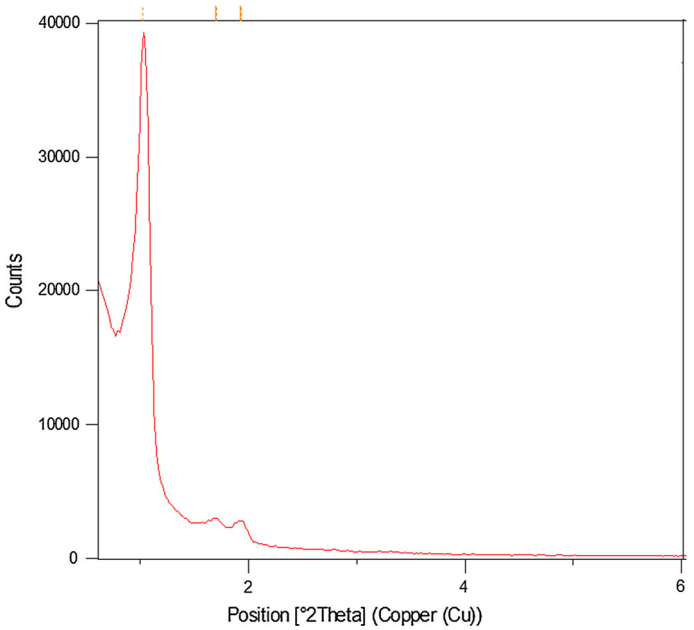

Fig. 6 The XRD patterns of VO-AMPD@SBA-15

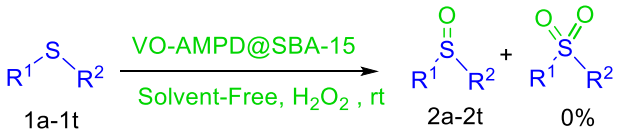

Scheme 2 VO-AMPD@SBA-15 catalyzed the oxidation of sulfides to sulfoxides

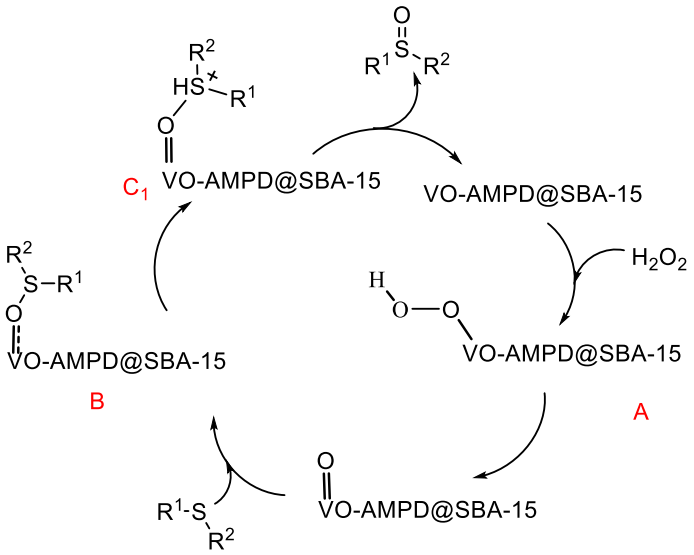

Scheme 3 Proposed mechanism for oxidation of sulfides in presence of VO-AMPD@SBA-15 as catalyst

methylphenylsulfide was selected as a model reaction. In order to optimize the reaction conditions, the effects of solvent, amount of catalyst and H_2O_2 were studied for the model reaction. Our observations are summarized in Table 2. Because of mild conditions of described heterogeneous systems, there is no overoxidation to sulfone for oxidation of sulfides.

In order to gain further insight into this process and with optimal conditions in hand, we also decided to examine the wider applicability of the catalyst for the oxidation of a wide range of sulfides with different functional groups. The results of the investigation are summarized in Table 3.

In continuation of this research work, a reaction mechanism for oxidation of sulfides in the presence of VO-AMPD@SBA-15 is proposed on the basis of the literature [25]. Initially, reaction of H_2O_2 with VO-AMPD@SBA-15 leads to the intermediate *A*. The intermediate *A* is converted to active oxidant *B* and then nucleophilic attack of the sulfide on this intermediate (C_1) produced corresponding sulfoxide (Fig. 7).

It should be mentioned that the catalytic activity of VO-AMPD complex in comparison with VO-AMPD@SBA-15 is investigated for the conversion of methylphenylsulfide to the methylphenylsulfoxide under optimized conditions. As

Table 2 Optimization of oxidation of sulfides to the corresponding sulfoxides using VO-AMPD@SBA-15 nanoparticles under various conditions

Entry	Solvent	H_2O_2 (mL)	Catalyst (mg)	Time (min)	Yield (%)[a]
1	Solvent-free	0.3	0	140	–[b]
2	Solvent-free	0.2	3	85	87
3	Solvent-free	0.3	4	60	98
4	Solvent-free	0.3	3	75	89
5	Solvent-free	0.3	5	55	98
6	Solvent-free	0.4	4	55	97
7	Solvent-free	0.5	4	50	91
8	Ethanol	0.3	4	85	90
9	Ethyl acetate	0.3	4	120	89
10	Acetonitrile	0.3	4	140	91

[a]Isolated yields

[b]Control experiment in the absence of catalyst

Table 3 Oxidation of sulfides to the corresponding sulfoxides in the presence of VO-AMPD@SBA-15

Entry	Substrate	Product	Time (min)	Yield (%)[a]
1	Dodecyl methylsulfide	2a	45	97
2	Dipropylsulfide	2b	35	98
3	Dibenzylsulfide	2c	25	97
4	Tetrahydrothiophene	2d	5	99
5	Propylenesulfide	2e	30	98
6	Diethylsulfide	2f	45	92
7	Ethylphenylsulfide	2g	20	97
8	Benzylmethylsulfide	2h	25	98
9	Diphenylsulfide	2i	20	96
10	Benzylphenylsulfide	2j	15	92
11	Bis(4-hydroxyphenyl)sulfide	2k	30	90
12	Dimethylsulfide	2l	50	93
13	Methylphenylsulfide	2m	60	98
14	Allyl(methyl)sulfide	2n	40	91
15	2-Furfurylmethylsulfide	2o	55	92
16	Dibutylsulfide	2p	50	89
17	4-Chlorophenyl(methyl) sulfide	2q	30	96
18	2-(Methylthio)ethanol	2r	45	90
19	*n*-Dodecylsulfide	2s	55	93
20	2-(Phenylthio)ethanol	2t	25	98

[a]Isolated yields

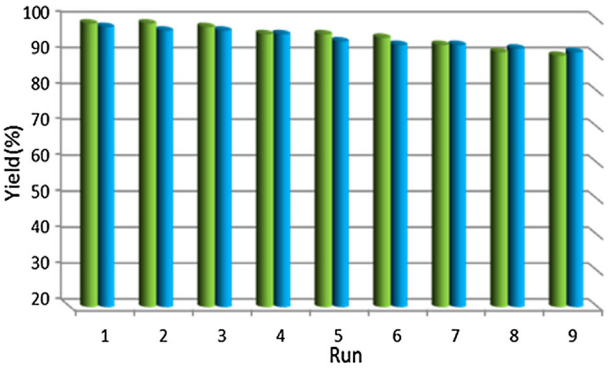

Fig. 7 Reusability of VO-AMPD@SBA-15 for the oxidation of tetrahydrothiophene (green column) and the oxidative coupling of 4-methylthiophenol (blue column). (Color figure online)

shown in Table 4, the products were obtained in 92 and 98% yield in the presence of VO-AMPD complex and VO-AMPD@SBA-15, respectively.

After successfully synthesizing a series of sulfoxides with high efficiency, the catalytic activity of VO-AMPD@SBA-15 was also investigated in the oxidative coupling of thiols. In order to optimize the reaction conditions, we investigated the oxidative coupling of 4-methylthiophenol as a model substrate in the absence and presence of various solvents and in the presence of different amounts of VO-AMPD@SBA-15 using different amounts of hydrogen peroxide (H_2O_2). The results of the investigation are summarized in Table 5.

With the optimal reaction conditions in hand, we extended the scope of the method for the wide range of aromatic and aliphatic thiols. The results of the chemoselective oxidation of thiols to disulfides are summarized in Table 6. It should be mentioned that the thiols afforded the corresponding products in short times with good to excellent yields (Scheme 4).

The proposed mechanism for this process using H_2O_2 as oxidant in the presence VO-AMPD@SBA-15 catalyst is outlined in Scheme 5 [24].

Recyclability of the catalyst

In addition, according to the green chemistry viewpoint, the recovery and reusability of catalyst is an outstanding issue in modern catalysis researches. In this regard, the

Table 4 Effect of VO-AMPD complex in comparison with VO-AMPD@SBA-15 in oxidation of methylphenylsulfide as a model compound under optimized conditions

Entry	Substrate	Catalyst	Time (min)	Catalyst (mg)	Yield (%)[a]
1	Methylphenylsulfide	VO-AMPD complex	60	4	92
2	Methylphenylsulfide	VO-AMPD@SBA-15	60	4	98 [this work]

[a]Isolated yields

Table 5 Optimization of oxidative coupling of thiols to disulfides using VO-AMPD@SBA-15 under various conditions

Entry	Solvent	H2O2 (mL)	Catalyst (mg)	Time (min)	Yield (%)[a]
1	Ethyl acetate	0.4	0	180	–[b]
3	Ethyl acetate	0.4	4	50	98
4	Solvent-free	0.4	3	70	87
5	Ethyl acetate	0.4	5	45	98
6	Ethyl acetate	0.3	4	65	90
7	Ethyl acetate	0.5	4	45	98
8	Ethanol	0.4	4	95	91
9	Solvent-free	0.4	4	70	93
10	Acetonitrile	0.4	4	85	89

[a]Isolated yields

[b]Control experiment in the absence of catalyst

Table 6 Oxidative coupling of thiols to disulfides using H_2O_2 in the presence of VO-AMPD@SBA-15

Entry	Substrate	Product	Time (min)	Yield (%)[a]
1	Mercaptosuccinic acid	4a	35	99
2	2-Mercaptobenzoic acid	4b	20	95
3	Phenylmethanethiol	4c	25	94
4	Benzo[d]thiazole-2-thiol	4d	45	97
5	4-Methylbenzenethiol	4e	50	98
6	2-Mercapto-6-methylpyridine	4f	40	96
7	Benzenethiol	4g	35	96
8	2-Mercaptopyridine	4h	65	92
9	2-Mercaptoacetic acid	4i	60	89
10	2,6-Dichlorobenzenethiol	4j	35	98
11	4-Mercaptopyridine	4k	70	93
12	4-Phenylimidazole-2-thiol	4l	30	95
13	4,6-Dimethyl-2-pyrimidinethiol	4m	35	90
14	2-Mercaptoethanol	4n	40	97
15	2-Mercaptoimidazole	4o	50	92
16	2-Aminothiophenol	4p	85	97
17	1-Ethyl-1H-imidazole-2-thiol	4q	80	98
18	4-Bromothiophenol	4r	30	90
19	Naphthalene-2-thiol	4s	25	93
20	Benzo[d]oxazole-2-thiol	4t	40	99

[a]Isolated yields

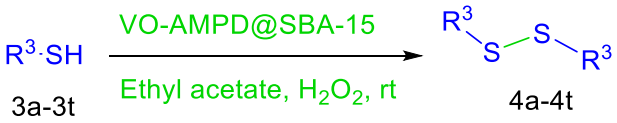

Scheme 4 VO-AMPD@SBA-15 catalyzed the oxidative coupling of thiols into disulfides

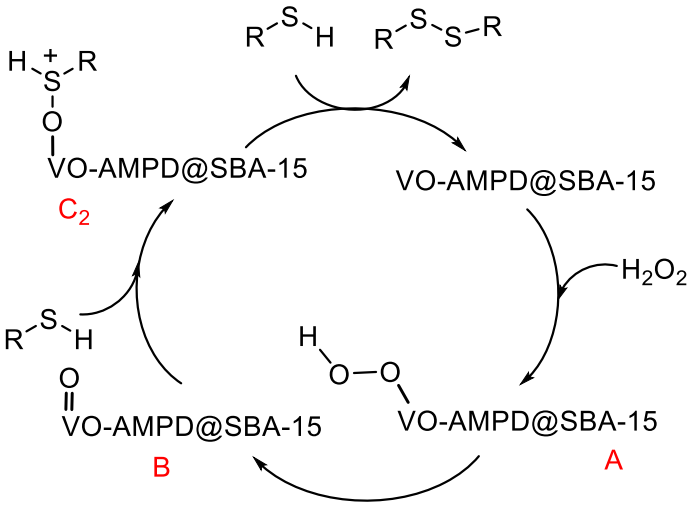

Scheme 5 Proposed mechanism for oxidative coupling of thiols in presence of VO-AMPD@SBA-15 as catalyst

prepared catalyst has the potential for efficient recycling for nine additional reaction cycles without significant loss of catalytic activity, establishing the reusability of the catalyst. As evident in Fig. 8, this experiment obviously proves that vanadium is covalently anchored to the organic functional groups on the SBA-15 nanostructure surface.

The nature of the recovered catalyst was investigated by EDX (Fig. 8) XRD patterns (Fig. 9), SEM (Fig. 10) and ICP-OES analysis. The results indicate that the catalyst can be recycled without any significant change in its structure or mesoporousity of the silicate parent.

The energy-dispersive X-ray spectroscopy (EDX) analysis of the recovered catalyst shows the presence of peaks associated with Si, O, N, C and V specie in the catalyst. In order to determine the exact amount of V loaded on modified SBA-15 nanoparticles, ICP-OES analysis of recovered catalyst was performed, and it was found to be 0.37 mmol g^{-1}. Therefore, the catalytic activity has been decreased slightly because the leaching of metal from VO-AMPD@SBA-15 is very negligible.

As seen in Fig. 9, the X-ray diffraction analysis (XRD) patterns of recovered catalyst were recorded by powder X-ray diffraction (XRD). It can be seen that the XRD pattern of the catalyst has not been changed in the recovered catalyst.

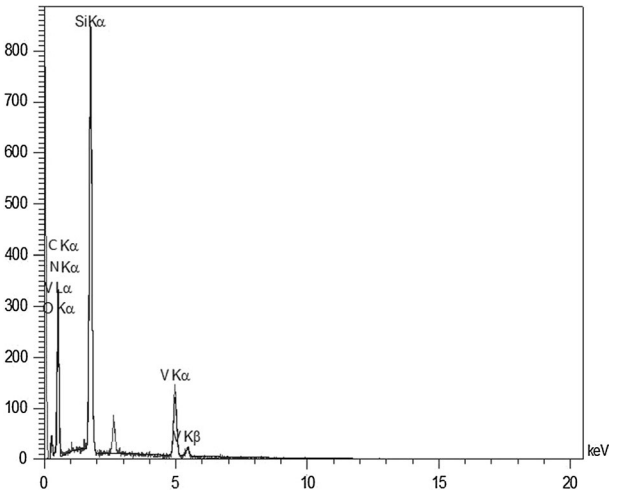

Fig. 8 EDX spectrum of recovered VO-AMPD@SBA-15

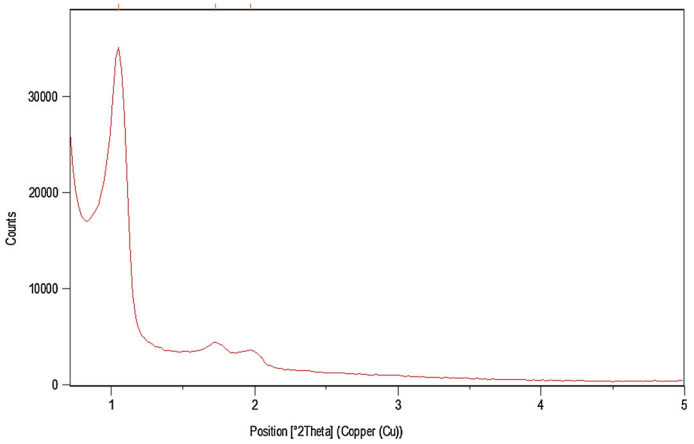

Fig. 9 The XRD patterns of recovered VO-AMPD@SBA-15

The morphology of the recovered VO-AMPD@SBA-15 was also obtained using the scanning electron microscopy (SEM) technique (Fig. 10).

Hot filtration test

Also, the oxidation of 4-methylbenzenethiol in the presence of VO-AMPD@SBA-15 has been investigated by carrying out a hot filtration test in order to find whether the catalyst is truly heterogeneous in nature or whether vanadium is leaching out from the solid catalyst to the solution. In this experiment, after continuing the reaction under optimized conditions, we found the yield of product in a half time of

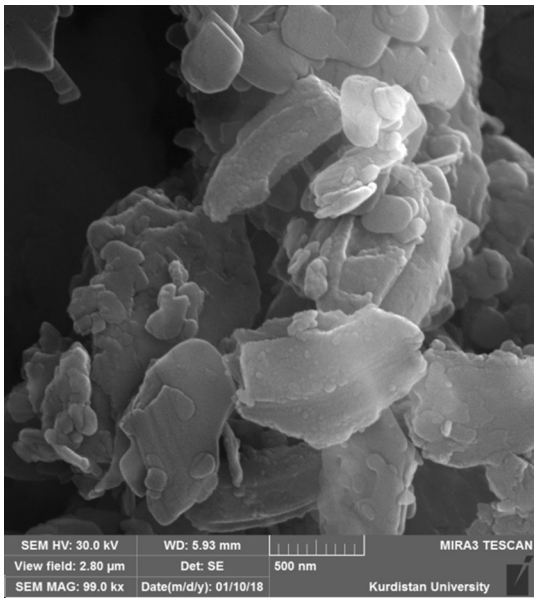

Fig. 10 SEM images of recovered VO-AMPD@SBA-15

the reaction to be 67%. Then the reaction was repeated and in a half time of the reaction, the catalyst was separated from the reaction mixture and allowed the filtrate to react further under identical reaction conditions. The yield of reaction in this stage was 73% that confirmed the leaching of vanadium had not occurred.

Comparison of the catalyst

In order to examine the efficiency of overall performance of the catalyst reactions, we compared the results of the synthesis of methylphenylsulfoxde in the presence of our catalyst with previously reported catalysts in the literature (Table 7). It should be noted that the prepared catalyst showed shorter reaction times, easier purification and better yields than the other catalysts. Also, in comparison with other catalysts, easy catalyst/product separation and catalyst recycling, easy preparation using cheap and commercially available materials in a short period of time, use of non-toxic ligands, easy separation, and stability are several benefits of this protocol.

Conclusion

In the present work, a VO-AMPD@SBA-15 nanohybrid was successfully obtained via a simple and versatile procedure, which was confirmed with FT-IR, TGA, SEM, ICP-OES, XRD, BET and TEM. Also, the performance of VO-AMPD@SBA-15 as an efficient, green and reusable catalyst for the oxidation of sulfides and oxidative coupling of thiols was investigated. The prepared catalytic system can combine the advantages of homogeneous and heterogeneous catalysts, and; therefore ,they can

Table 7 Comparison of VO-AMPD@SBA-15 for the oxidation of methylphenylsulfide with previously reported procedures

Entry	Catalyst	Time (min)	Yield (%)[a]
1	$(CH_3)_4N^+CrO_3F^-$	75	82 [26]
2	Alumina-supported nanoruthenium/H_2O_2	120	92 [27]
3	$2NaBO_3{\cdot}4H_2O$(I)/KBr	120	57 [18]
4	Thiourea dioxide/TBHP	210	93 [28]
5	SiO_2–W2–Py/H_2O_2	150	90 [29]
6	$(C_2H_5)_3NH^+[CrO_3F]^-$	120	84 [30]
8	Ni(II)-Salen-MCM-41/UHP	155	95 [17]
9	Borax/H_2O_2	360	92 [31]
10	Cd(II)-Salen-MCM-41/UHP	150	98 [17]
11	Clay-supported ceric ammonium nitrate (CAN)/O_2	300	35 [32]
12	Iron(II)-catalyzed	120	94 [33]
13	VO-AMPD@SBA-15	60	98 [this work]

[a]Isolated yields

be readily separated from the solution by simple filteration, allowing straightforward recovery and reuse. More importantly, this method offers several advantages including the use of commercially available materials, short reaction times, clean reactions, operational simplicity, high efficiency under relatively mild conditions, a waste-free process, and cheap and chemically stabile reagents.

Acknowledgements The authors are deeply grateful to Erfan Ghadermazi, University of Kurdistan and Ilam University for financial support of this research project.

References

1. A. Masahiko, Z. Fengyu, Catalyst **5**, 868 (2015)
2. F. Havasi, A. Ghorbani-Choghamarani, F. Nikpour, Microporous Mesoporous Mater. **224**, 26 (2016)
3. C.E. Song, J.S. Lim, S.C. Kim, K. Lee, D.Y. Chi, Chem. Commun. **24**, 2415 (2000)
4. T. Tamoradi, A. Ghorbani-Choghamarani, M. Ghadermazi, New J. Chem. **41**, 11714 (2017)
5. M.A. Zolfigol, V. Khakyzadeh, A.R. Moosavi-Zare, A. Zare, P. Arghavani-Hadi, Z. Mohammadi, M.H. Beyzavi, J Chem. **65**, 280 (2012)
6. M. Darabi, T. Tamoradi, M. Ghadermazi, A. Ghorbani-Choghamarani, Transit Metal Chem. **42**, 703 (2017)
7. S. Shylesh, V. Schunemann, W.R. Thiel, Angew. Chem. Int. Ed. **49**, 3428 (2010)
8. P. Movaheditabar, M. Javaherian, V. Nobakht, React. Kinet. Mech. Catal. **122**, 217 (2017)
9. C.W. Lim, I.S. Lee, Nano Today **5**, 412 (2010)
10. J. Kulys, R. Vidziunate, J. Mol, Catal. B Enzym. **37**, 79 (2005)
11. D. Zhao, J. Feng, Q. Hou, N. Melosh, G.H. Fredrickson, B.F. Chmelka, G.D. Stucky, Science **279**, 548 (1998)
12. X.B. Li, Z.J. Li, Y.J. Gao, Q.Y. Meng, S. Yu, R.G. Weiss, G.H. Tung, L.Z. Wu, Angew. Chem. Int. Ed. **53**, 2085 (2014)
13. E. Rattanangkool, W. Krailat, T. Vilaivan, P. Phuwapraisirisan, M. Sukwattanasinitt, S. Wacharasindhu, Eur. J. Org. Chem. **22**, 4795 (2014)
14. H.B. Jeon, K.T. Kim, S.H. Kim, Tetrahedron Lett. **55**, 3905 (2014)

15. A. Shaabani, A.H. Rezayan, Catal. Commun. **8**, 1112 (2007)
16. A. Sreedhar, P. Radhika, B. Neelima, N. Hebalkar, A.K. Mishra, Catal. Commun. **10**, 39 (2008)
17. M. Nikoorazm, A. Ghorbani-Choghamarani, H. Mahdavi, S. Mostaffa Esmaeili, Microporous Mesoporous Mater. **211**, 174 (2015)
18. D. Habibi, M.A. Zolfigol, M. Safaiee, A. Shamsian, A. Ghorbani-Choghamarani, Catal. Commun. **10**, 1257 (2009)
19. H. Firouzabadi, N. Iranpoor, M. Abbasi, Tetrahedron Lett. **51**, 508 (2010)
20. Y. Liu, H. Wang, C. Wang, J.P. Wan, C. Wen, RSC Adv. **3**, 21369 (2013)
21. J. Davarpanah, A.R. Kiasat, Catal. Commun. **46**, 75 (2014)
22. A. Ghorbani-Choghamarani, B. Tahmasbi, P. Moradi, Appl. Organometal. Chem. **30**, 422 (2016)
23. M. Nikoorazm, A. Ghorbani-Choghamarani, M. Khanmoradi, Appl. Organometal. Chem. **30**, 236 (2016)
24. M. Hajjami, F.Ghorbani, Z. Yousofvand, Appl. Organometal. Chem. 2017
25. T. Tamoradi, M. Ghadermazi, A. Ghorbani-Choghamarani, Appl. Organometal. Chem. 2017
26. H. Imanieh, S. Ghamami, M.K. Mohammadi, A. Jangjoo, Russ. J. Gen. Chem. **77**, 282 (2007)
27. P. Veerakumar, Z. Lu, M. Velayudham, K.L. Lu, S. Rajagopal, J. Mol. Catal. A **332**, 128 (2010)
28. S. Kumar, S. Verma, S.L. Jain, B. Sain, Tetrahedron Lett. **52**, 3393 (2011)
29. S. Xian-Ying, W. Jun-Fa, J. Mol. Catal. A Chem. **280**, 142 (2008)
30. S. Ghammamy, M.K. Mohammadi, A.H. Joshaghani, Maced. J. Chem. Chem. Eng. **27**, 117 (2008)
31. S. Hussain, S.K. Bharadwaj, R. Pandey, M.K. Chaudhuri, Eur. J. Chem. **42**, 3319 (2009)
32. A. Dhakshinamoorthy, K. Pitchumani, Catal. Commun. **10**, 872 (2009)
33. B. Li, A.H. Liu, L.N. He, Z.Z. Yang, J. Gao, K. Hong, ChenGreenChem **14**, 130 (2012)